Critical behavior at nematic–smectic-A phase transitions

Carl W. Garland and George Nounesis*
Center for Materials Science and Engineering and Department of Chemistry, Massachusetts Institute of Technology, Cambridge, Massachusetts 02139
(Received 6 December 1993)

The effective experimental critical exponents α, γ, $\nu_{\|}$, and $\nu_{\perp}$ obtained from high-resolution heat capacity and x-ray studies of nematic–smectic-A transitions in liquid crystals are presented as a function of the ratio T_{NA}/T_{NI} of the nematic–smetic-A transition temperature to that of the nematic-isotropic transition. These results, which are the most extensive ever reviewed, show complex systematic trends that are compared with the theoretically predicted crossover from three-dimensional XY to tricritical behavior and the anisotropic behavior predicted to arise due to coupling between the smectic order parameter and director fluctuations.

PACS number(s): 64.70.Md, 61.30.−v, 64.60.Fr

I. INTRODUCTION

The nematic (N)–smectic-A (Sm-A) transition has been the most extensively studied of all liquid-crystal phase transitions. The nematic phase is an orientationally ordered but translationally disordered phase with rodlike molecules aligned with their long axes parallel to the director **n**. The smectic-A phase contains layers (one-dimensional translational order) with the normal to the layers parallel to the director; i.e., the long axes of molecules in a layer are perpendicular to the layer. Since de Gennes first pointed out in 1972 the close analogy between the N–Sm-A transition and the normal-superconducting phase transition in metals [1], there has been great interest in the critical behavior at this transition. Although the N–Sm-A transition would seem to represent a simple kind of one-dimensional freezing, it has proved to be one of the most challenging, as yet unsolved, problems in the statistical mechanics of condensed matter.

During the past twenty years, many high-resolution heat-capacity and x-ray studies have been devoted to the N–Sm-A transition [2–34]. These studies were aimed at determining the critical exponents α for the heat capacity C_p, γ for the order-parameter susceptibility χ, and $\nu_{\|}$ and $\nu_{\perp}$ for the correlation lengths $\xi_{\|}$ and $\xi_{\perp}$ parallel and perpendicular to the normal to the smectic layers. In addition, optical studies have also been made of the Frank twist-and-bend elastic constants K_2 and K_3 in the nematic phase [35–38] and the compressional elastic constant B in the smectic phase [39–41]. The result of these experiments has been a wide range of effective critical exponents that do not agree with the values expected from the 3D-XY ($d=3$, $n=2$ vector model) universality class.

The theory of the N–Sm-A transition has also received considerable attention [42–50]. The simplest model would involve an isotropic 3D-XY fixed point governing the asymptotic behavior, with corrections-to-scaling terms needed in the preasymptotic regime [51,52], since that regime is accessed experimentally. This model gives a good description of C_p, χ, and the correlation volume $\xi_{\|}\xi_{\perp}^2$ for compounds with very large nematic ranges, but does not account for the weak critical anisotropy ($\nu_{\|}\neq\nu_{\perp}$) observed in the correlation lengths [32]. Large nematic range should correspond to large values of the splay elastic constant K_1. In the limit where $K_1\rightarrow\infty$, gauge transformation theory [45] predicts that the XY fixed point is unstable. However, effective critical behavior that is weakly anisotropic might be observed in a nonasymptotic experimental regime [45]. In the opposite limit, where $K_1\rightarrow 0$, theory predicts that the N–Sm-A transition is like that in a type-II superconductor with $\nu_{\|}=\nu_{\perp}=\nu_{XY}$ but with inverted heat-capacity amplitude ratios [43,45]. However, calorimetric studies that yield critical exponents $\alpha=\alpha_{XY}$ also yield amplitude ratios inconsistent with this inverted XY model [25]. It should also be noted that Monte Carlo simulations of N–Sm-A transitions give noninverted C_p peaks [47]. The anisotropy in the critical behavior of $\xi_{\|}$ and $\xi_{\perp}$, which arises due to the finite splay stiffness $0<K_1<\infty$, has been treated by dislocation-loop melting theory [44], gauge transformation theory [45], and self-consistent one-loop theory [49,50].

Recent experiments on the N–Sm-A_1 and N–Sm-A_2 transitions of compounds exhibiting monolayer Sm-A_1 and bilayer Sm-A_2 phases [30–34] and recent theoretical predictions of Patton and Andereck [49,50] provide a stimulus to review the trends in effective critical exponents that have been reported experimentally. Partial descriptions of such trends have been given previously [15,53,54]. Clear if somewhat complicated patterns emerge from the experimental data. Although not all outstanding issues are resolved, the overall experimental

*Present address: Francis Bitter National Magnet Laboratory, MIT, Cambridge, MA 02139.

behavior can be understood qualitatively and provides a starting point for further theoretical work.

II. EFFECTIVE CRITICAL EXPONENTS

The most reliable critical exponents α, γ, $\nu_\parallel$, and $\nu_\perp$ determined in the nematic phase near N–Sm-A transitions are given in Table I, arranged in order of increasing MacMillan ratio T_{NA}/T_{NI} (i.e., decreasing nematic range). These exponent values were typically determined from experimental data over the reduced temperature range $2\times10^{-5}<t<10^{-2}$, where $t=(T-T_c)/T_c$. The smectic susceptibility and correlation lengths were fitted with pure power laws,

$$\chi=\chi_0 t^{-\gamma},\quad \xi_\parallel=\xi_{\parallel 0}t^{-\nu_\parallel},\quad \xi_{\perp 0}t^{-\nu_\perp}; \tag{1}$$

while the excess heat capacity $\Delta C_p=C_p-C_p$(background) has been fitted with the form

$$\Delta C_p^{\pm}=A^{\pm}|t|^{-\alpha}\left[1+D_1^{\pm}|t|^{\Delta_1}\right]+B_c\ , \tag{2}$$

where B_c is the critical contribution to the regular (nonsingular) term and the corrections-to-scaling exponent Δ_1 is set equal to the XY value 0.524 [51] or to the essentially equivalent value 0.5. Heat-capacity data are available both above and below T_c, and the data analysis involved simultaneous fits to $\Delta C_p^{\pm}$ with $\alpha^+=\alpha^-=\alpha$. Since typically 300–500 data points were available for ΔC_p, range shrinking [13,25] could be carried out and the necessity

TABLE I. Effective critical exponents obtained from heat-capacity and x-ray studies of second-order nematic–smectic-A transitions. The nature of the smectic phase is indicated: A_m for nonpolar monomeric smectics, A_1 for polar monolayer smectics, A_d for partial bilayer smectics, and A_2 for bilayer smectics. The chemical structures corresponding to the common symbolic names are given in Table II. Typical uncertainties in the experimental values are ±(0.02–0.05) for α, ±(0.05–0.06) for γ, and ±(0.03–0.05) for $\nu_\parallel$ and $\nu_\perp$.

Material	Type	T_{NA}/T_{NI}	α	γ	$\nu_\parallel$	$\nu_\perp$	Ref.
3DXY			−0.007	1.316	0.669	0.669	[51]
T8	A_1	0.660	XY	1.26	0.70	0.65	[22,32]
T7	A_1	0.706	XY	1.23	0.69	0.61	[22,32]
DB5+C_5 stilbene	A_1	0.780	XY	1.30	0.73	0.57	[24,25,32]
DB_8ONO_2	A_1	0.808	XY	1.28	0.69	0.59	[31,32]
DB6+TBBA[a]	A_1	0.810		1.36	0.72	0.52	[19]
DB6	A_d	0.820	b	1.29	0.67	0.52	[19]
7APCBB	A_2	0.863	XY	1.34	0.70	0.64	[28,34]
D6.1AOB	A_m	0.889	XY	1.24	0.75	0.65	[29]
8OPCBOB	A_1	0.898	XY	1.39	0.71	0.56	[26,30,32]
$\overline{7.7}$S5[c]	A_m	0.916	b	1.52	0.82	0.68	[16]
6OCB+8OCB[d]	A_d	0.920	b	1.49	0.76	0.62	[10,18]
$\overline{6}O\overline{9}$	A_m	0.923		1.45	0.78	0.68	[21]
$\overline{4O.7}$	A_m	0.926	−0.03	1.46	0.78	0.65	[15]
$\overline{7.8}$S5[c]	A_m	0.927	~0	1.45	0.81	0.68	[16]
CBOOA[e]	A_d	0.934	0.15	1.3–1.5	0.70	0.62	[2-4,8]
$\overline{8}$S5	A_m	0.936	~0	1.53	0.83	0.68	[5,11]
7.6CB	A_d	0.953	−0.03	1.38	0.82	0.58	[17,33]
8.5S5	A_m	0.954	0.10	1.48	0.78	0.66	[20]
4O.8	A_m	0.958	0.13	1.31	0.70	0.57	[12,23]
8OCB	A_d	0.963	0.20	1.32	0.71	0.58	[8,9,12]
$\overline{9}$S5	A_m	0.967	0.22	1.31	0.71	0.57	[6,20]
8CB	A_d	0.977	0.31	1.26	0.67	0.51	[7,13,20]
$\overline{9.8}$S5	A_m	0.981	0.40	1.22	0.66	0.53	[20]
$\overline{10}$S5	A_m	0.983	0.45	1.10	0.61	0.51	[6,20]
EEBAC	A_m	0.991		1.23	0.71	0.45	[14]
9CB[f]	A_d	0.994	0.50	1.09	0.57	0.37	[17,20]
9.04CB[f]	A_d	0.995		1.07	0.54	0.38	[20]
Tricritical			0.5	1.0	0.5	0.5	[1]

[a]This mixture containing 18 mol % TBBA is considered to be far enough removed from the N–Sm-A_1–Sm-A_2 point at ~12 mol % TBBA to be unaffected by that multicritical point.

[b]C_p measurements have been made, but the excess heat capacity ΔC_p is too small to permit evaluation of α.

[c]$\overline{7.x}$S5 represents a mixture of $\overline{7}$S5 and $\overline{8}$S5, with $0.x$ being the mole fraction of $\overline{8}$S5. The N–Sm-A–Sm-C point lies at $\overline{7.57}$S5, and $\overline{7.7}$S5 as well as $\overline{7.85}$S5 are considered far enough removed to be unaffected by that multicritical point.

[d]This mixture contains 25 mol % 6OCB. For mixtures with a 6OCB mole percent greater than 30 there is no stable Sm-A phase. The quoted exponents are obtained with a phenomenological extension of optimal density theory; see Ref. [18].

[e]This compound is included for the sake of completeness in spite of the fact that the measurements were very early ones (mid 1970s) and the critical exponents are less certain than those for the other materials. CBOOA exponents are not plotted in Figs. 1–3.

[f]According to the calorimetric data in Ref. [17], 9CB is close to the tricritical point but very weakly first order. The estimated tricritical mixture is 8.96 CB.

of retaining corrections-to-scaling terms has been confirmed in many cases. For N–Sm-A_1 and N–Sm-A_2 transitions in materials with large nematic ranges, when α was allowed to be a free parameter, its value was always close to zero and statistically equivalent fits were obtained with α fixed at the XY value of -0.007 [25–28]. For N–Sm-A_d and N–Sm-A_m transitions in materials with moderately large nematic ranges, ΔC_p becomes very small (or even undetectable) and no α exponent can be determined [10].

The systems listed in Table I represent a comprehensive set of all "simple" second-order N–Sm-A transitions known to the authors. The structures and chemical names of these materials are given in Table II. Not included in Table I are systems near special regions in the phase diagram or multicritical points other than the tricritical point. Omitted are data near the N–Sm-A–Sm-C point (such as $\overline{7}$S5+$\overline{8}$S5 and $\overline{7}$S5+8OCB), data where Fisher renormalization occurs due to steep phase boundaries ($\overline{7}$S5+8OCB and 8OCB + TBBA), data near the reentrant nose of a N–Sm-A_d–N_r curve (6OCB +8OCB), data near the N–Sm-A_1–SmA_2 point (DB6+TBBA), and data from reentrant nematic (N_r) lakes or estuaries having the Sm-A_d–N_r–Sm-A_1 sequence (DB_8ONO_2+$DB_{10}ONO_2$ and 11.O.NCS + 10 OPCBOB). All of these systems involve special complications that are understood at least in general terms, and such systems are not helpful to establishing the pattern for normal N–Sm-A behavior.

The exponents in Table I are plotted versus the ratio T_{NA}/T_{NI}, where T_{NA} is the nematic-smectic-A critical temperature and T_{NI} is the first-order nematic-isotropic transition temperature. Since $(T_{NI}-T_{NA})/T_{NI}=1-T_{NA}/T_{NI}$, this ratio is a direct measure of the width of the nematic range. The thermodynamic exponents α and γ are shown in Fig. 1, and the correlation exponents $\nu_\parallel$ and $\nu_\perp$ are shown in Fig. 2. Also shown is a plot of $\nu_\parallel+2\nu_\perp$ values in Fig. 3. This quantity represents the effective critical exponent for the correlation volume $\xi_\parallel\xi_\perp^2$. In each case, the isotropic 3D-XY exponent values [51], $\alpha=-0.007$, $\gamma=1.316$, $\nu=0.669$, $3\nu=2.007$, are indicated by a horizontal dashed line.

III. DISCUSSION

It is clear from Figs. 1–3 that the experimental effective critical exponents show a complicated but systematic pattern as a function of T_{NA}/T_{NI}. This ratio is a necessarily crude measure of two important sources of deviations from isotropic 3D-XY behavior.

The first type of deviation involves crossover from a second-order to a first-order transition via a Gaussian tricritical point. This behavior occurs due to coupling between the smectic order parameter Ψ and the nematic orientational order parameter S [1]. When the nematic range is narrow and the orientational susceptibility is large, this coupling can drive the coefficient b of the Ψ^4 term in the free-energy negative, which leads to a first-order N–Sm-A transition. Tricritical behavior occurs at the point where the coefficient $b=0$.

The second type of deviation from isotropic XY behavior is due to the coupling between director fluctuations δn and the smectic order parameter Ψ [45,49]. We shall stress here the self-consistent one-loop theory of Patton and Andereck [49,50], which does not utilize the gauge transformation approach used by Lubensky [45]. This coupling is intrinsically anisotropic and the Patton-Andereck model predicts a very gradual crossover in the behavior from isotropic to a broad weakly anisotropic critical correlation regime (weak coupling) to strongly anisotropic ($\nu_\parallel=2\nu_\perp$) behavior in the strong-coupling limit. Numerical solutions [50] for a set of bare parameter

TABLE II. Chemical structures for various smectic materials together with their commonly used symbolic names. The phenyl group is denoted by ϕ. Replacement of the integer n by $n.x$ represents a mixture of two homologs, n and $n+1$, with x being the mole fraction of the higher homolog.

Symbolic name	Chemical structure
	Nonpolar
$\overline{n}$Sm	C_nH_{2n+1}—O—ϕ—COS—ϕ—C_mH_{2m+1}
$\overline{n}$O$\overline{m}$	C_nH_{2n+1}—O—ϕ—COO—ϕ—O—C_mH_{2m+1}
nO.m	C_nH_{2n+1}—O—ϕ—CH=N—ϕ—C_mH_{2m+1}
DnAOB	C_nH_{2n+1}—ϕ—NO=N—ϕ—C_nH_{2n+1}
EEBAC	C_2H_5—O—ϕ—CH=N—ϕ—CH=CH—$COOC_2H_5$
TBBA	C_4H_9—ϕ—N=CH—ϕ—CH=N—ϕ—C_4H_9
	Polar
nCB	C_nH_{2n+1}—ϕ—ϕ—CN
nOCB	C_nH_{2n+1}—O—ϕ—ϕ—CN
CBOOA	C_8H_{17}—ϕ—N=CH—ϕ—CN
n.O.NCS	C_nH_{2n+1}—O—ϕ—COO—ϕ—NCS
DBn or DB$_n$CN	C_nH_{2n+1}—ϕ—OOC—ϕ—OOC—ϕ—CN
$C_n$stilbene	C_nH_{2n+1}—ϕ—CH=CH—ϕ—OOC—ϕ—CN
DB_nONO_2	C_nH_{2n+1}—O—ϕ—OOC—ϕ—OOC—ϕ—NO_2
Tn	C_nH_{2n+1}—O—ϕ—COO—ϕ—CH=CH—ϕ—CN
nOPCBOB	C_nH_{2n+1}—O—ϕ—OOC—ϕ—O—CH_2—ϕ—CN
nAPCBB	C_nH_{2n+1}—OOC—ϕ—OOC—ϕ—OOC—ϕ—CN

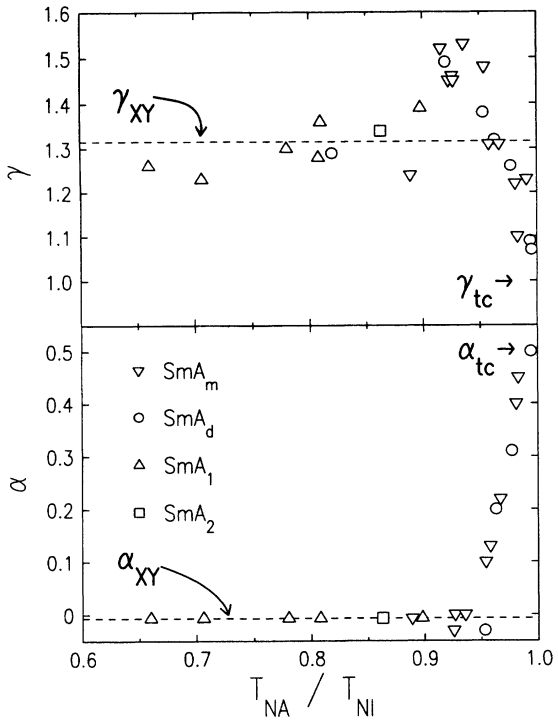

FIG. 1. Thermodynamic effective critical exponents α and γ. The isotropic 3D-XY values of $\alpha_{XY}=-0.007$ and $\gamma_{XY}=1.316$ are indicated by the dashed lines, and the tricritical values $\alpha_{tc}=0.5$ and $\gamma_{tc}=1.0$ are indicted by small arrows. Crossover from second order to tricritical is limited to the range $T_{NA}/T_{NI}>0.93$.

values $K_{30}/K_{20}=3$, $K_{30}/K_1=2$, and $\xi_{\parallel 0}/\xi_{\perp 0}=7$) typical of polar liquid-crystal systems show that crossover extends over ~ 8 orders of magnitude in reduced temperature, as shown in Fig. 4. The theoretical variable a/a_{30} is proportional to t^{γ}. Thus for $\gamma=\gamma_{XY}=1.316$, the 11 decades between $a/a_{30}=10^4$ and 10^{-7} correspond to ~ 8 decades in t. Note that the weakly anisotropic regime from $a/a_{30}=10^4$ to 10^{-2} (where $\nu_\perp<\nu_{\text{isotropic}}$ but $\nu_\parallel\simeq\nu_{\text{isotropic}}$) corresponds to ~ 4 decades in t, and the further crossover to the strongly anisotropic regime takes another ~ 4 decades in t. Since experimental correlation lengths are typically available over less than three decades in reduced temperature, we take the view that experimental effective exponents $\nu_\parallel$ and $\nu_\perp$ represent average values over a short part of the very broad crossover range.

The strength of the coupling between the director fluctuation and the order parameter, and thus the position of the accessible experimental reduced temperature range within the a/a_{30} crossover regime will depend on the magnitude of the splay elastic constant K_1. Generally speaking, the Frank elastic constants K_i vary as the square of the nematic order parameter S [1,49]. Thus materials with small nematic ranges will have small K_1 values at T_{NA} and should lie deeper into the anisotropic crossover. In contrast to this, materials with large nematic ranges will have large K_1 values and should straddle the isotropic and weak-anisotropic regimes. The theoretical anisotropic crossover behavior shown in Fig. 4 can be compared with the experimental variation of $\nu_\parallel/\gamma$ and $\nu_\perp/\gamma$ as a function of T_{NA}/T_{NI} given in Fig. 5. The effective exponent behavior in Figs. 1–3 clearly indicates that tricritical crossover effects occur in the range $0.93<T_{NA}/T_{NI}<1$. Thus let us consider primarily the ν/γ behavior in Fig. 5 for $T_{NA}/T_{NI}<0.93$, where the Gaussian tricritical fixed point should not influence the results. Comparison with Fig. 4 suggests these systems are in the weak-coupling regime where $\nu_\parallel/\gamma$ is constant and $\nu_\perp/\gamma$ exhibits a dip. The plateau value $\nu_\perp/\gamma\approx 0.45$ for $T_{NA}/T_{NI}\geq 0.8$ agrees fairly well with the theoretical

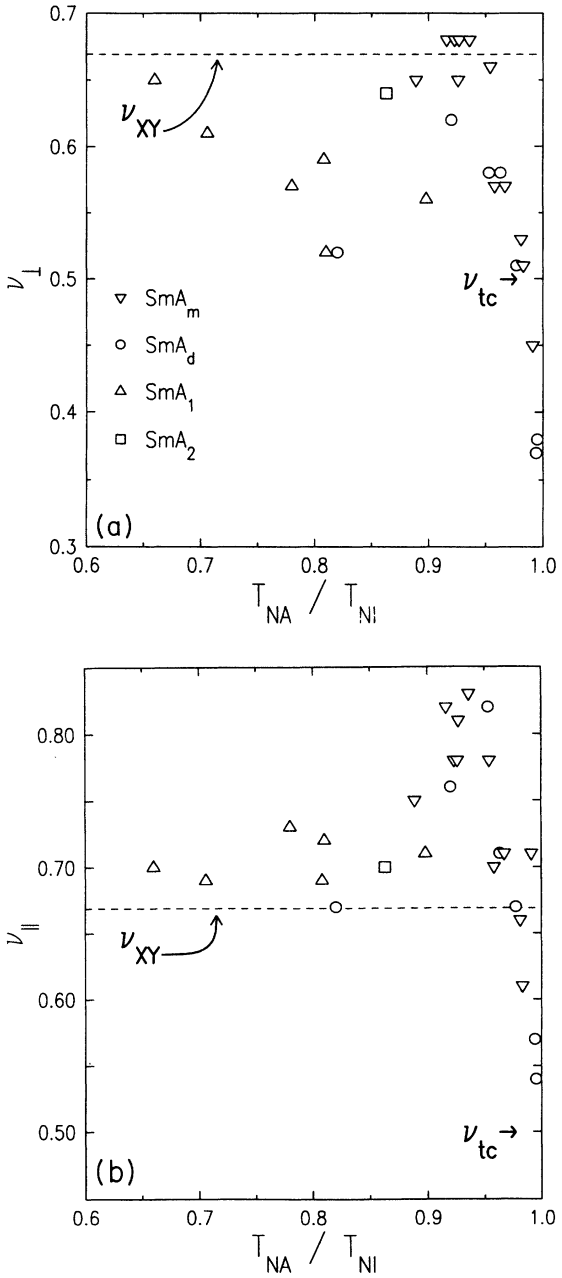

FIG. 2. Effective correlation exponents (a) $\nu_\perp$ and (b) $\nu_\parallel$. The horizontal dashed line represents $\nu_{XY}=0.669$. As in Fig. 1, tricritical crossover occurs in the range $T_{NA}/T_{NI}>0.93$, and the tricritical exponent value $\nu_{tc}=0.5$ is indicated by the small arrows.

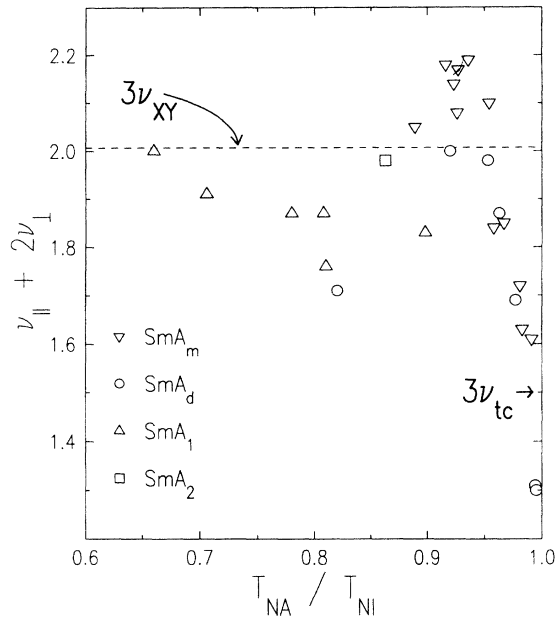

FIG. 3. Effective exponent $\nu_{\parallel}+2\nu_{\perp}$ describing the critical behavior of the correlation volume $\xi_{\parallel}\xi_{\perp}^2$. The dashed line is $3\nu_{XY}=2.007$.

prediction $\nu_{\perp}/\gamma=0.42$ at $a/a_{30}\simeq 5\times 10^{-2}$. For the range $0.93<T_{NA}/T_{NI}<1$) one expects tricritical (tc) crossover and possibly stronger anisotropy but there is no available theory for simultaneous δn-ψ and S-Ψ coupling effects. In the simplest view, anisotropy would be completely due to δn-Ψ coupling and the Patton-Andereck model might give qualitatively correct predictions for $\nu_{\parallel}/\gamma$ and $\nu_{\perp}/\gamma$ even when γ crossovers over from $\gamma_{XY}=1.316$ to $\gamma_{tc}=1.0$. If this view is valid, then strong anisotropy is never realized in these experimental systems (since $\nu_{\parallel}/\gamma$ does not rise toward 2) and furthermore a/a_{30} is not a monotonic function of T_{NA}/T_{NI} in the range $\sim 0.9<T_{NA}/T_{NI}\leq 1$.

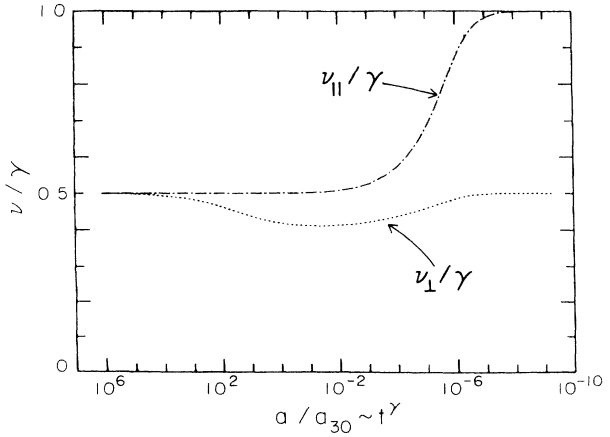

FIG. 4. Variation of theoretical $\nu_{\parallel}/\gamma$ and $\nu_{\perp}/\gamma$ effective exponent values as a function of the theoretical variable a/a_{30} (which is proportional to t^{γ}) according to the self-consistent one-loop theory of Patton and Andereck [49,50]. This figure, taken from Ref. [50], is based on a typical set of model parameters (see text).

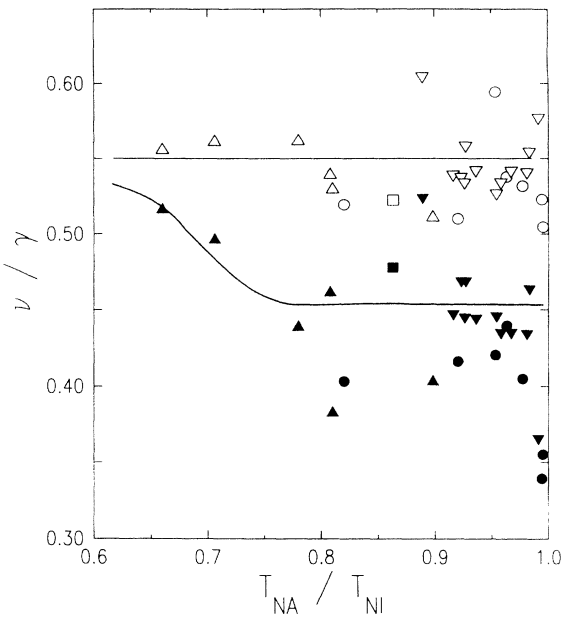

FIG. 5. Variation of experimental $\nu_{\parallel}/\gamma$ and $\nu_{\perp}/\gamma$ ratios of effective critical exponents as a function of the McMillan parameter T_{NA}/T_{NI}. The lines are merely guides for the eye. Open symbols are $\nu_{\parallel}/\gamma$ and solid symbols are $\nu_{\perp}/\gamma$. △ and ▲ for Sm-A_1, □ and ■ for Sm-A_2, ○ and ● for Sm-A_d, ▽ and ▼ for Sm-A_m.

A. Heat capacity

The heat-capacity behavior is in good agreement with 3D-XY predictions for all samples with $T_{NA}/T_{NI}\leq 0.93$. This agreement includes not only the value of the critical exponent α but all the universal amplitude ratios expected for a 3D-XY system [25,32]. In particular, the experimental amplitude ratios $A^-/A^+\simeq 0.99\pm 0.004$ are in good agreement with the 3D-XY universal value $A^-/A^+=0.9714\pm 0.0126$ [52] and are inconsistent with an inverted-XY value of 1.0294; see Ref. [25] for a detailed discussion of this point. Thus the theoretical prediction of inverted 3D-XY behavior at the N–Sm-A transition [43] is not supported by experimental data over the accessible reduced temperature range.

When the nematic range becomes short, i.e., $T_{NA}/T_{NI}\gtrsim 0.93$, the expected crossover to tricritical behavior is observed. This crossover for C_p has been observed in many systems that are not included in Table I since x-ray data are not available [55,56]. The T_{NA}/T_{NI} value at the tricritical point and the crossover curve of α_{eff} vs T_{NA}/T_{NI} are not universal, but data for different homologous series follow very similar trends [17,54–56].

B. Smectic susceptibility

The order-parameter susceptibility is obtained from the intensity of diffuse x-ray scattering in the nematic phase. Data for systems with $T_{NA}/T_{NI}\geq 0.93$ show γ crossing over toward the tricritical value of 1.0. Systems with large nematic ranges, $T_{NA}/T_{NI}<0.88$, exhibit effective γ values that are close to or lower than γ_{XY} when γ_{eff} is obtained from a pure power-law fit. Howev-

er, internal consistency requires that corrections-to-scaling terms must play a role in the susceptibility expression whenever they are important for the heat capacity. Analysis of the four N–SM-A_1 systems with $T_{NA}/T_{NI}<0.81$ shows that preasymptotic 3D isotropic XY theory represents the susceptibility data well using correction terms completely determined by the C_p data, i.e., there are no freely adjustable parameters associated with the susceptibility correction terms [32]. Neglect of such preasymptotic correction terms in the isotropic XY model can be shown to generate effective exponents $\gamma_{\rm eff}<\gamma_{XY}$. Thus the γ values in Fig. 1 for $T_{NA}/T_{NI}\lesssim 0.85$ are unaffected by tricritical or anisotropic coupling terms and can be well described by 3D-XY theory.

An empirical feature of the γ-vs-T_{NA}/T_{NI} curve in Fig. 1 that deserves special comment is the set of ten γ values *greater than* γ_{XY} that are observed for systems with $0.88<T_{NA}/T_{NI}<0.96$. There does not seem to be at present any theoretical model that predicts such behavior. The gauge theory of Lubensky [45] does not predict well-defined values for γ, and it is estimated in the self-consistent one-loop theory [50] that director fluctuations do not play a role in renormalizing γ over the weakly anisotropic region. However, the data in Fig. 1 clearly indicate that γ rises above γ_{XY} before crossover toward tricriticality occurs.

C. Correlation lengths

The $\nu_\perp$ behavior in Fig. 2(a) can be viewed as a composite of two effects: anisotropy due to coupling to director fluctuations and tricritical crossover due to Ψ-S coupling. The Patton-Andereck prediction for the anisotropy effect can be calculated from Fig. 4 if we assume $\gamma=\gamma_{XY}$, which seems to be valid at least for systems with $T_{NA}/T_{NI}\lesssim 0.85$. The resulting $\nu_\perp$ values vary from $\nu_\perp=\gamma/2\simeq\nu_{XY}$ in the isotropic regime, where coupling to director fluctuations has a negligible effect, to $\nu_\perp\simeq 0.54$ for the weak-anisotropy regime (value calculated for a typical set of model parameters). In the strong-coupling region, the prediction is $\nu_\perp=\gamma/2$ but γ is not well known theoretically. Since the necessary Frank elastic constants are unknown for the materials with $T_{NA}/T_{NI}<0.9$, the precise position in terms of T_{NA}/T_{NI} for the minimum in $\nu_\perp$ is uncertain. However, the general agreement in the range of magnitudes for experimental and theoretical $\nu_\perp$ values in the weak-coupling regime is encouraging. One puzzling feature of Fig. 2(a) should be noted. Although tricritical crossover occurs for $T_{NA}/T_{NI}>0.93$ as expected from the α and γ behavior, the last three $\nu_\perp$ values associated with the largest T_{NA}/T_{NI} ratios are *less than* the Gaussian tricritical value of 0.5. The reason for this is unclear, but no theory has yet attempted to deal simultaneously with both δn-ψ and ψ-S coupling to produce a theory of anisotropic tricritical crossover.

The effective $\nu_\parallel$ values shown in Fig. 2(b) exhibit a distinctly different type of deviation from the 3D-XY value than that observed for $\nu_\perp$. It should be stressed that the self-consistent one-loop theoretical curve for $\nu_\parallel$ shown in Fig. 4 is based on the same model parameters as were used for $\nu_\perp$. Note that predicted deviations from $\nu_\perp=\gamma_{XY}/2\simeq\nu_{XY}$ do not begin until the middle of the weak-anisotropy region. One of the significant features of the Patton-Andereck model is the prediction that deviations of $\xi_\parallel$ and $\xi_\perp$ from isotropic XY behavior first occur at quite different reduced temperatures for a given $\delta n-\psi$ coupling strength or, conversely, at different coupling strengths for a given experimental range of reduced temperature values [49,50].

The experimental $\nu_\parallel$ values for systems with $T_{NA}/T_{NI}\leq 0.81$ lie systematically above the expected ν_{XY} values, but these differences may not be significant in view of the typical uncertainty of ± 0.03 in $\nu_\parallel$ values. As T_{NA}/T_{NI} increases from ~ 0.8 to ~ 0.93, the experimental $\nu_\parallel$ values increase significantly and then crossover toward tricritical behavior occurs in the range $0.93<T_{NA}/T_{NI}<1$, as it does for all the critical exponents. It appears that one cannot access experimentally the strongly anisotropic second-order regime (where $\nu_\parallel=2\nu_\perp$) associated with strong δn-ψ coupling in the Patton-Andereck model. Indeed, as indicated in Fig. 5, the behavior of $\nu_\parallel^{\rm eff}$ is very well correlated to that of $\gamma^{\rm eff}$ over the entire range of T_{NA}/T_{NI}. One does *not* see a trend toward $\nu_\parallel\to 1$ as $\gamma\to 1$ (which would arise from $\nu_\parallel/\gamma=1$) as one might expect from the simplest view of a highly anisotropic tricritical point. Indeed, Fig. 5 shows that $\nu_\parallel^{\rm eff}/\gamma^{\rm eff}\simeq 0.55$ is a useful empirical generalization. This yields $(2-\eta_\parallel^{\rm eff})=\gamma^{\rm eff}/\nu_\parallel^{\rm eff}\simeq 1.82$ or $\eta_\parallel^{\rm eff}\simeq 0.18$ instead of $\eta_{XY}=0.03$ over a wide range of T_{NA}/T_{NI}. For the largest nematic ranges, where we believe $\gamma=\gamma_{XY}$ and $\nu_\parallel+2\nu_\perp=3\nu_{XY}$ when correction terms are property taken into account, this $\eta_\parallel^{\rm eff}$ empirical value implies that $\nu_\parallel\simeq 0.72$ and $\nu_\perp\simeq 0.64$ as a consequence of δn-ψ coupling.

D. Correlation volume

Figure 3 shows the behavior of $\nu_\parallel+2\nu_\perp$, which characterizes the critical variation of the correlation volume $\xi_\parallel\xi_\perp^2$. These exponent values were obtained, as usual, from pure power-law fits to the correlation volume data. Let us consider in more detail the region represented by systems with $0.66\leq T_{NA}/T_{NI}\leq 0.81$. In this range, the effective $\nu_\parallel+2\nu_\perp$ values all lie below $3\nu_{XY}$, as one would expect for an isotropic XY model when corrections-to-scaling terms play a significant role. It is known from all heat-capacity analyses that corrections-to-scaling terms are required to describe the ΔC_p data. In the case of materials with long nematic ranges, the ΔC_p data are well described by exact solutions of preasymptotic 3D-XY isotropic theory [32]. In this case, the magnitude of the heat-capacity correction-term amplitude D_1^+ depends on the value of a nonuniversal temperature scaling parameter θ_0. Compared to other XY systems, such as helium near its lambda transition, the value of θ_0 is relatively large for polar liquid crystals with large nematic ranges. Thus, to be internally consistent, one should consider the role of corrections-to-scaling terms for the susceptibility and correlation volume. The magnitude of such correc-

tion terms all depend on the single parameter θ_0, which can be determined from heat-capacity analysis and used without further adjustment for analysis of χ and $\xi_\parallel\xi_\perp^2$. Analysis of the four N–Sm-A_1 systems with $T_{NA}/T_{NI}<0.81$ shows that the behavior of $\xi_\parallel\xi_\perp^2$ can be well represented by preasymptotic 3D isotropic XY theory using $\nu_\parallel+2\nu_\perp=3\nu_{XY}$ [32]. Thus hyperscaling $\nu_\parallel+2\nu_\perp=2-\alpha$ is obeyed, and furthermore there is good agreement for the product of nonuniversal amplitudes A^+ and $(\xi_\parallel\xi_\perp^2)_0$ with the two-scale-factor universal value for the XY model [32]. This assumption that one can use isotropic XY theory for the correlation volume is clearly *ad hoc* since anisotropy in $\xi_\parallel$ and $\xi_\perp$ is observed for these systems. However, the idea that the description of the correlation volume may be close to that of isotropic theory even when the individual correlation lengths are anisotropic does not seem unreasonable in view of the direct relation between $\xi_\parallel\xi_\perp^2$ and the free energy per unit volume via two-scale-factor universality. In this view, the δn-ψ coupling could be the source of large correction terms for $\xi_\parallel\xi_\perp^2$, which are then reflected in large correction terms for the heat capacity and susceptibility behavior.

IV. CONCLUSION

The effective critical exponents α, γ, $\nu_\parallel$, and $\nu_\perp$ for N–Sm-A transitions exhibit complicated but systematic trends as a function of the McMillan ratio T_{NA}/T_{NI}. This parameter represents a convenient but imprecise measure of the strength of two important couplings: the ψ-S coupling between the smectic and nematic order parameters that gives rise to crossover toward a tricritical point and an eventual first-order transition when T_{NA}/T_{NI} is very close to 1, and the δn-ψ coupling between the director fluctuations and the smectic order parameter that gives rise to anisotropic behavior for the correlation lengths.

The tricritical crossover affects all of the critical exponents and becomes dominant in the range $0.93\lesssim T_{NA}/T_{nI}\lesssim 1$. This complicates the theory of δn-ψ coupling in a regime where that coupling is expected to become stronger. However, it is unlikely that K_1 in any experimental system ever gets sufficiently small so that the Patton-Andereck strong-coupling limit (where $\nu_\parallel=2\nu_\perp$) can be realized. This view is supported by the fact that for a given homologous series the N-I transition becomes more strongly first order as $T_{NA}/T_{NI}\to 1$ [56]. Thus K_1 should jump discontinuously at T_{NI} to a significant value in the nematic phase. It also follows from this view of K_1 behavior that the type-II superconductor fixed point associated with $K_1\to 0$ does not play any role in liquid-crystal N–Sm-A critical behavior. A proper theory for materials with $T_{NA}/T_{NI}\geq 0.93$ will require simultaneous treatment of both ψ-S and δn-ψ coupling leading to anisotropic crossover from second-order behavior to a Gaussian tricritical behavior that may still exhibit anisotropy.

By studying materials with large nematic ranges, say, $T_{NA}/T_{NI}<0.81$, one can avoid the effects of ψ-S coupling, but weak anisotropy still occurs for the correlation lengths, especially $\xi_\perp$, which is more influenced by δn-ψ coupling than $\xi_\parallel$. For these materials, the heat capacity and smectic susceptibility can be well described by preasymptotic versions of isotropic XY theory in which first-order corrections-to-scaling terms play an important role [32]. It should be stressed that, for ΔC_p data over the accessible reduced temperature range, the amplitude ratio A^-/A^+ agrees with the normal XY value and is inconsistent with the inverted-XY value.

It also appears empirically that the correlation volume for materials with $T_{NA}/T_{NI}<0.81$ can be described in a self-consistent manner using the same preasymptotic isotropic theory. One challenge for future theory is to explore the connection between anisotropic $\xi_\parallel$ and $\xi_\perp$ behavior and pseudoisotropic $\xi_\parallel\xi_\perp^2$ behavior, including a link between the magnitude of the correction terms for $\xi_\parallel\xi_\perp^2$ and those for χ and C_p. Another theoretical challenge is to provide an explanation for effective γ values greater than γ_{XY}. An experimental challenge is to measure the Frank elastic constants for splay (K_1), twist (K_2), and bend (K_3) in the materials with large nematic ranges. The Patton-Andereck model [50] makes predictions for the anisotropic renormalization of the elastic constants K_2 and K_3 that could be tested experimentally. Note in particular that both the one-loop and gauge transformation theories predict a different onset of the crossover behavior for δK_2 and δK_3 than that predicted for the correlation lengths. Thus comparison of effective δK exponents with effective ξ exponents must be done with caution. However, in the one-loop model the underlying correlation lengths determined indirectly from the Frank elastic constants should agree with those measured directly with x rays, which is in contrast to gauge-dependent differences predicted by gauge transformation theories [45]. The available experimental evidence on this point from materials with larger T_{NA}/T_{NI} values [15,35,53] favors the agreement predicted from the self-consistent one-loop theory.

For materials with T_{NA}/T_{NI} values in the intermediate range 0.81–0.93, the experimental situation is more complex and the theoretical situation is less clear. Heat-capacity data continue to conform well to isotropic XY behavior, but the susceptibility exponent γ rises from $\gamma_{XY}=1.316$ to ~ 1.55 before crossover toward tricritical begins. This γ_{eff} behavior is not predicted by any of the present models. For the correlation behavior, there is considerable scatter in the $\nu_\parallel$ and $\nu_\perp$ trends, some aspects of which agree with anisotropic Patton-Andereck predictions. Note that this range of T_{NA}/T_{NI} values involves an overlap of data from different types of smectic-A materials—both Sm-A_m and Sm-A_d materials which comprise all of the systems with large T_{NA}/T_{NI} values and Sm-A_1 and Sm-A_2 materials that dominate at small T_{NA}/T_{NI} values.

ACKNOWLEDGMENTS

The authors would like to thank B. S. Andereck, R. J. Birgeneau, T. C. Lubensky, and B. R. Patton for many helpful discussions. This work was supported by National Science Foundation Grants Nos. DMR 90-07611, DMR 90-22933, and DMR 93-11853.

[1] P. G. deGennes, Solid State Commun. **10**, 753 (1972); Mol. Cryst. Liq. Cryst. **21**, 49 (1973); *The Physics of Liquid Crystals* (Clarendon, Oxford, 1974).
[2] W. L. McMillan, Phys. Rev. A **7**, 1419 (1973).
[3] D. Djurek, J. Baturic-Rubcic, and K. Franulovic, Phys. Rev. Lett. **33**, 1126 (1974).
[4] J. Als-Nielsen, R. J. Birgeneau, M. Kaplan, J. D. Litster, and C. R. Safinya, Phys. Rev. Lett. **39**, 352 (1977); **41**, 1626 (E) (1978).
[5] C. A. Schantz and D. L. Johnson, Phys. Rev. A **17**, 1504 (1978).
[6] P. Brisbin, R. DeHoff, T. E. Lockhart, and D. L. Johnson, Phys. Rev. Lett. **43**, 1171 (1979).
[7] D. Davidov, C. R. Safinya, M. Kaplan, S. S. Dana, R. Schaetzing, R. J. Birgeneau, and J. D. Litster, Phys. Rev. B **19**, 1656 (1979).
[8] J. D. Litster, J. Als-Nielsen, R. J. Birgeneau, S. S. Dana, D. Davidov, F. Garcia-Golding, M. Kaplan, C. R. Safinya, and R. Schaetzing, J. Phys. (Paris) Colloq. **40**, C3-339 (1979).
[9] C. W. Garland, G. B. Kasting, and K. J. Lushington, Phys. Rev. Lett. **43**, 1420 (1979); G. B. Kasting, K. J. Lushington, and C. W. Garland, Phys. Rev. B **22**, 321 (1980); I. Hatta and N. Nokayama, Mol. Cryst. Liq. Cryst. **66**, 417 (1981); J. M. Viner and C. C. Huang, Solid State Commun. **39**, 789 (1981).
[10] K. J. Lushington, G. B. Kasting, and C. W. Garland, Phys. Rev. B **22**, 2569 (1980).
[11] C. R. Safinya, R. J. Birgeneau, J. D. Litster, and M. E. Neubert, Phys. Rev. Lett. **47**, 668 (1981).
[12] R. J. Birgeneau, C. W. Garland, G. B. Kasting, and B. M. Ocko, Phys. Rev. A **24**, 2624 (1981).
[13] J. Thoen, H. Marynissen, and W. Van Dael, Phys. Rev. A **26**, 2886 (1982).
[14] A. Rajewska, B. Pura, and J. Przedmojski, J. Phys. (Paris) **43**, 1669 (1982).
[15] C. W. Garland, M. Meichle, B. M. Ocko, A. R. Kortan, C. R. Safinya, J. J. Yu, J. D. Litster, and R. J. Birgeneau, Phys. Rev. A **27**, 3234 (1983).
[16] C. R. Safinya, Ph.D. thesis, Massachusetts Institute of Technology, 1981 (unpublished).
[17] H. Marynissen, J. Thoen, and W. van Dael, Mol. Cryst. Liq. Cryst. **97**, 149 (1983); J. Thoen, H. Marynissen, and W. van Dael, Phys. Rev. Lett. **52**, 204 (1984).
[18] A. R. Kortan, H. von Känel, R. J. Birgeneau, and J. D. Litster, J. Phys. (Paris) **45**, 529 (1984).
[19] K. K. Chan, P. S. Pershan, L. B. Sorensen, and F. Hardouin, Phys. Rev. Lett. **54**, 1694 (1985); Phys. Rev. A **34**, 1420 (1986).
[20] B. M. Ocko, R. J. Birgeneau, and J. D. Litster, Z. Phys. B **62**, 487 (1986).
[21] B. M. Ocko, Ph.D. thesis, Massachusetts Institute of Technology, 1984 (unpublished).
[22] K. W. Evans-Lutterodt, J. W. Chung, B. M. Ocko, R. J. Birgeneau, C. Chiang, C. W. Garland, E. Chin, J. Goodby, and N. H. Tinh, Phys. Rev. A **36**, 1387 (1987).
[23] K. J. Stine and C. W. Garland, Phys. Rev. A **39**, 3148 (1989).
[24] K. Ema, C. W. Garland, G. Sigaud, and N. H. Tinh, Phys. Rev. A **39**, 1369 (1989).
[25] C. W. Garland, G. Nounesis, and K. J. Stine, Phys. Rev. A **39**, 4919 (1989).
[26] C. W. Garland, G. Nounesis, K. J. Stine, and G. Heppke, J. Phys. (Paris) **50**, 2291 (1989).
[27] G. Nounesis, C. W. Garland, and R. Shashidhar, Phys. Rev. A **43**, 1849 (1991).
[28] X. Wen, C. W. Garland, and G. Heppke, Phys. Rev. A **44**, 5064 (1991).
[29] L. Chen, J. D. Brock, J. Huang, and S. Kumar, Phys. Rev. Lett. **67**, 2037 (1991); S. Kumar (private communication).
[30] W. G. Bouwman and W. H. de Jeu, Phys. Rev. Lett. **68**, 800 (1992).
[31] G. Nounesis, K. I. Blum, M. J. Young, C. W. Garland, and R. J. Birgeneau, Phys. Rev. E **47**, 1910 (1993).
[32] C. W. Garland, G. Nounesis, M. J. Young, and R. J. Birgeneau, Phys. Rev. E **47**, 1918 (1993).
[33] W. B. Bouwman and W. H. de Jeu, J. Phys. I (to be published).
[34] L. Wu, M. J. Young, Y. Shao, C. W. Garland, and R. J. Birgeneau, Phys. Rev. Lett. **72**, 376 (1994).
[35] S. Sprunt, L. Solomon, and J. D. Litster, Phys. Rev. Lett. **53**, 1923 (1984).
[36] R. Mahmood, D. Brisbin, I. Khan, C. Gooden, A. Baldwin, D. L. Johnson, and M. E. Neubert, Phys. Rev. Lett. **54**, 1031 (1985).
[37] C. Gooden, R. Mahmood, D. Brisbin, A. Baldwin, D. L. Johnson, and M. E. Neubert, Phys. Rev. Lett. **54**, 1035 (1985).
[38] H. K. M. Vithana, G. Xu, and D. L. Johnson, Phys. Rev. E **47**, 3441 (1993).
[39] M. R. Fisch, L. B. Sorensen, and P. S. Pershan, Phys. Rev. Lett. **48**, 943 (1982).
[40] M. R. Fisch, P. S. Pershan, and L. B. Sorensen, Phys. Rev. A **29**, 2741 (1984).
[41] M. Benzakri, T. Claverie, J. P. Marcerou, and J. C. Rouillon, Phys. Rev. Lett. **68**, 2480 (1992).
[42] B. I. Haperin, T. C. Lubensky, and S. K. Ma, Phys. Rev. Lett. **32**, 292 (1974).
[43] C. Dasgupta and B. I. Halperin, Phys. Rev. Lett. **47**, 1556 (1981).
[44] D. R. Nelson and J. Toner, Phys. Rev. B **24**, 363 (1981); J. Toner, *ibid.* **26**, 462 (1982).
[45] T. C. Lubensky, J. Chim. Phys. **80**, 31 (1983), and references therein; (private communication).
[46] J. Prost, Adv. Phys. **33**, 1 (1984).
[47] C. Dasgupta, J. Phys. (Paris) **48**, 957 (1987).
[48] P. Barois, J. Pommier, and J. Prost, in *Solitons in Liquid Crystals,* edited by L. Lam and J. Prost (Springer-Verlag, Berlin, 1989).
[49] B. R. Patton and B. S. Andereck, Phys. Rev. Lett. **69**, 1556 (1992).
[50] B. S. Andereck and B. R. Patton, Phys. Rev. E **49**, 1393 (1994).
[51] C. Bagnuls and C. Bervillier, Phys. Rev. B **32**, 7209 (1985); see also C. Bagnuls, C. Bervillier, D. I. Meiron, and B. G. Nickel, *ibid.* **35**, 3585 (1987).
[52] C. Bagnuls and C. Bervillier, Phys. Lett. A **112**, 9 (1985); C. Bervillier, Phys. Rev. B **34**, 8141 (1986).
[53] D. L. Johnson, J. Chim. Phys. **80**, 45 (1983).
[54] W. G. Bouwman and W. H. de Jeu, in *Modern Topics in Liquid Crystals,* edited by A. Buka (World Scientific, London, 1993).
[55] M. E. Huster, K. J. Stine, and C. W. Garland, Phys. Rev. A **36**, 2364 (1987), and references therein.
[56] J. Thoen, in *Phase Transitions in Liquid Crystals,* Vol. 290 of *NATO Advanced Study Institute, Series B: Physics,* edited by S. Martellucci and A. N. Chester (Plenum, New York, 1992), pp. 155–174.